Weak ferromagnetism in manganese tartrate dihydrate $MnC_4H_4O_6{\cdot}2H_2O$

2000 J. Phys.: Condens. Matter 12 2071

(http://iopscience.iop.org/0953-8984/12/9/311)

J. Phys.: Condens. Matter **12** (2000) 2071–2078. Printed in the UK PII: S0953-8984(00)09442-X

Weak ferromagnetism in manganese tartrate dihydrate $MnC_4H_4O_6 \cdot 2H_2O$

A Paduan-Filho† and C C Becerra

Instituto de Física, Universidade de São Paulo, CP 66318, São Paulo, SP, Brazil

E-mail: apaduan@if.usp.br

Received 10 November 1999

Abstract. Magnetization and differential susceptibility of manganese tartrate dihydrate were measured in a single crystal from room temperature down to 0.4 K and in the presence of magnetic fields up to 70 kOe. Nearly antiferromagnetic order occurs below $T_N = 1.83$ K, with spins oriented close to the c axis. Sharp peaks in the susceptibility and the presence of a remanent magnetization in the plane perpendicular to the c axis suggest a weak ferromagnetic structure of spins with a canting angle $\approx 0.6^\circ$. The magnetic phase diagram below T_N was determined. The exchange and anisotropy field were obtained respectively as $H_E = 19.4$ kOe and $H_A = 0.6$ kOe.

1. Introduction

The interest in the coordination of metals atoms with the tartrate group has been mainly linked with the ferroelectric and piezoelectric properties that members of this family exhibit [1]. The general chemical formula of these tartrate compounds is $XC_4H_4O_6$, where X can be a divalent ion (Zn, Mn, Ca, Cd, Gd etc) or it can be replaced by two monovalent ions (Na, Li, K, H, NH_4 etc). These compounds can also be grown with two, three and even four water molecules. Some members of this family (cadmium, calcium, sodium–ammonium, ammonium–ammonium) are ferroelectric [1–3] or piezoelectric [4] and there are compounds (sodium–potassium, rubidium–hydrogen, ammonium–hydrogen) used for transducer and many linear and non-linear devices [1]. $NaKC_4H_4O_6 \cdot 4H_2O$ was one of the first materials where ferroelectric properties were observed [5]. Surprisingly very few works were dedicated to the study of compounds of the tartrate group with transition metal ions, particularly to their magnetic properties. The only known works are those referring to the thermal and electromagnetic behaviour of manganese [6], calcium [2] and zinc tartrate [7].

Certain kinds of substance that are basically antiferromagnetic, can exhibit a small spontaneous moment perpendicular to the easy axis of antiferromagnetic alignment. This moment has its origin in a small canting of the spins of the sub-lattices [8, 9]. This weak ferromagnetic behaviour is linked as in the case of the ferroelectric properties with the absence of a centre of symmetry in the lattice [10, 11].

In this paper we report on the magnetic properties of manganese tartrate dihydrate, $MnC_4H_4O_6 \cdot 2H_2O$ (hereafter denoted MnT-2). Because of the non-centrosymmetric structures of the tartrate groups around the metal ions [1, 6], a weak ferromagnetic component is expected

† Addressee for correspondence: Professor Armando Paduan-Filho, Instituto de Física, Universidade de São Paulo, Caixa postal 66318, São Paulo, CEP 05315-970, Brazil.

0953-8984/00/092071+08$30.00

to occur in this compound. Apart from very old and incomplete magnetic studies in transition metal tartrate compounds [12] this paper is one of the first to present a magnetic study of a tartrate of the transition metal group.

2. Experimental details

The literature concerning manganese tartrate crystallographic structure is inconclusive. The same lattice parameters and spatial group have been reported for the compound with two, three and four water molecules [13–15]. Since details of the crystal structure of the Mn compound are unknown we have to rely on the reported structure from some supposedly isomorphous compounds such as cadmium tartrate [1] that has two molecules per unit cell. For our experiments we prepared large single crystals of manganese tartrate. They were grown from saturated water solutions, prepared through reaction of tartaric acid and manganese carbonate. Samples prepared with D and L tartaric acid were grown and gave identical magnetic results. During the growth process the solution was kept at a temperature of 55 °C. Thermogravimetric analysis of our samples showed that the loss of mass occurring between 90 and 200 °C was consistent with two water molecules per unit formula. Thus our samples are of the general formula $MnC_4H_4O_6 \cdot 2H_2O$. Well formed pink crystals ($4 \times 4 \times 5$ mm^3) with typical mass of 50 mg were used in the experiments. Based on the grown habit of the crystals we could identify the three crystallographic axes by measurements of the angles between the faces.

Magnetization measurements were done in a superconductor quantum interference device (SQUID) for temperatures above 2 K and up to 290 K. Some measurements between 1.7 K and 7 K were done using a vibrating sample magnetometer (VSM). Differential ac susceptibility (χ_{ac}) was measured in the temperature range from 0.4 to 7 K, with a mutual inductance Hartshorn bridge. In this set-up we operated with a modulation field of 1 Oe at a frequency of 155 hertz. High fields, up to 70 kOe, were obtained with a superconductor coil and low fields were produced by a copper solenoid. Temperatures below 1.2 K were obtained with a ^{3}He refrigerator [16, 17].

3. Results in low field

In the range of temperature from 2 to 290 K, dc molar susceptibility ($\chi_{dc} = M/H$) was obtained measuring the magnetization in a field of 100 Oe with the SQUID magnetometer. Data for reciprocal susceptibility $(\chi_{dc})^{-1}$ as a function of temperature are shown in figure 1. These data are for a sample in the powder form. For temperature above 5 K the curve can be fitted to a Curie–Weiss law $\chi_{dc} = C/(T + \theta)$, with parameters $C = 4.38$ K mol^{-1} and $\theta = 2.72 \pm 0.05$ K. The theoretical Curie constant $C = Ng^2\mu_B^2 S(S+1)/3k = 1.094g^2$ yields a spectroscopic factor $g = 2.00 \pm 0.02$. This value is the expected one for the manganese ion in the S state with spin 5/2. The positive value of θ indicates an antiferromagnetic exchange interaction among the Mn ions.

The ac susceptibility χ_{ac} for three perpendicular directions of a single crystal was measured below 5 K. Figure 2 shows data obtained when modulation field was applied along the b axis and c axis respectively. The data obtained from measurements in the a^* direction (perpendicular to the bc plane) (not shown) are very similar to those obtained along the b axis. Along the c axis χ_{ac} was measured down to 0.4 K. The susceptibility decreases below 1.83 K and tends to zero for very low temperatures. This is the expected behaviour for the parallel χ_{ac} for an antiferromagnet with long range order below $T_N = 1.83$ K. The c direction corresponds then to the easy antiferromagnetic axis. In the a^* and b direction χ_{ac} shows a sharp spike at T_N.

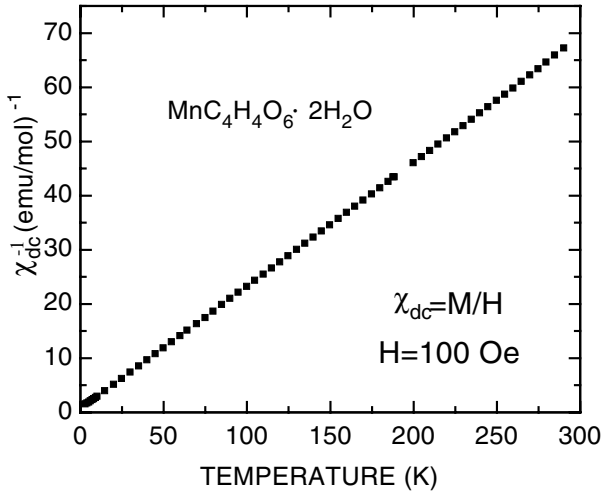

Figure 1. Plot of the reciprocal measured powder dc susceptibility of manganese tartrate dihydrate, as a function of temperature. The susceptibility fitted to a Curie–Weiss law $\chi_{dc} = C_m/(T + \theta)$ yields the parameters $C_m = 4.38$ K mol^{-1} and $\theta = 2.72$ K.

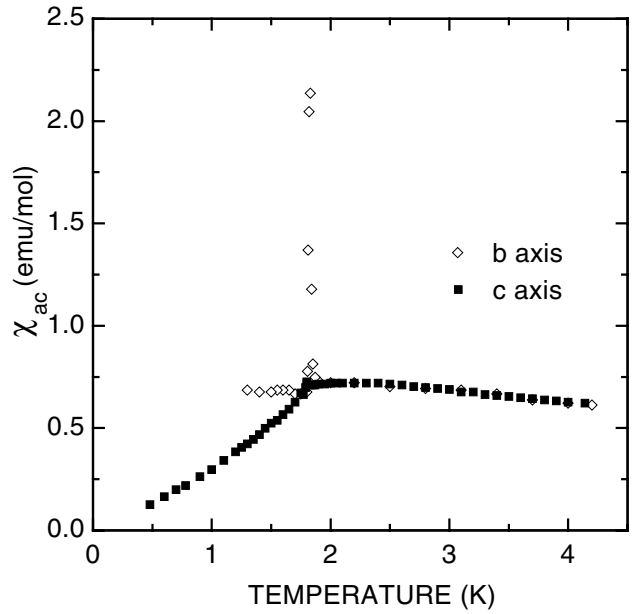

Figure 2. Ac susceptibilities measured parallel (c axis) and perpendicular (b axis) to the easy direction of magnetization for a single crystal of $MnC_4H_4O_6 \cdot 2H_2O$.

Below 1.7 K both perpendicular susceptibilities stabilize at a value of 0.71 emu mol^{-1}. The only difference between χ_{ac} data along directions b and a^* is in the height of the peak at T_N. The peaks in the two directions perpendicular to the easy axis are characteristic of the presence of a small ferromagnetic component along these directions. A slight misalignment of the anti-parallel magnetic sub-lattices with respect to the c axis can lead to a canting with

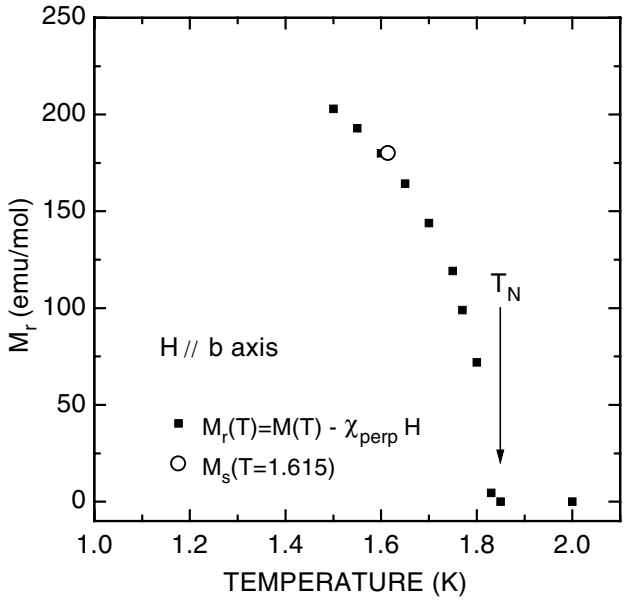

Figure 3. Remanent magnetization M_r obtained after the subtraction of the perpendicular susceptibility contribution to the magnetization. The sample was cooled in the presence of a constant applied field of 40 Oe. The M_s value obtained from the hysteresis curve in figure 4 is also indicated (○).

a net component in the ba^* plane. According to Dzyaloshinski [8] and Moriya [9] (DM), canting may occur only if the magnetic moments in a unit cell are not related by a centre of symmetry. In MnT-2 the existence of two manganese ions per unit cell surrounded by tartrate groups with non-centrosymmetric structures occurs, and this can result in the observed weak ferromagnetic component. If a dc magnetic field is applied along these directions it is observed that the height of the peak in the ac susceptibility decreases and that is suppressed for fields exceeding 40 Oe (because of a complete saturation of the weak component). Measurements along directions, other than b and a^*, perpendicular to the c axis also showed that the peak at T_N is still present. These peaks at T_N were predicted by Moriya [9] and observed in many weak ferromagnets [18].

The spontaneous weak magnetization along the two principal directions perpendicular to the easy axis was measured as a function of the temperature. In these experiments the sample was cooled in a constant applied field of 40 Oe to ensure a complete saturation of the weak component. The overall perpendicular magnetization should be represented by $M(T) = M_r(T) + \chi_{ac}H$, where $M_r(T)$ corresponds to the remanent net moment, and the linear term in H corresponds to the contribution of the perpendicular susceptibility. As the applied field increases, $M_r(T)$ should increase initially but it will saturate when the saturation value of the weak component $M_s(T)$ is attained. Only the antiferromagnetic susceptibility term $\chi_{ac}H$ will increase linearly with H afterwards. In figure 3 the obtained $M_s(T)$ after subtraction of the antiferromagnetic contribution ($\chi_{ac}H$) is plotted for the sample cooled in a field of $H = 40$ Oe applied along the b axis. Similar measurements were made with the cooling field of 40 Oe applied along the a^* direction. A small difference between the saturation value $M_s(T)$ along a^* and b directions was observed. These experiments permit the statement of a spontaneous moment $M_s(T)$ in the ba^* plane of the crystal for temperature below T_N. Considering that the behaviour of $M_s(T)$ as a function of T is the same as in other three-

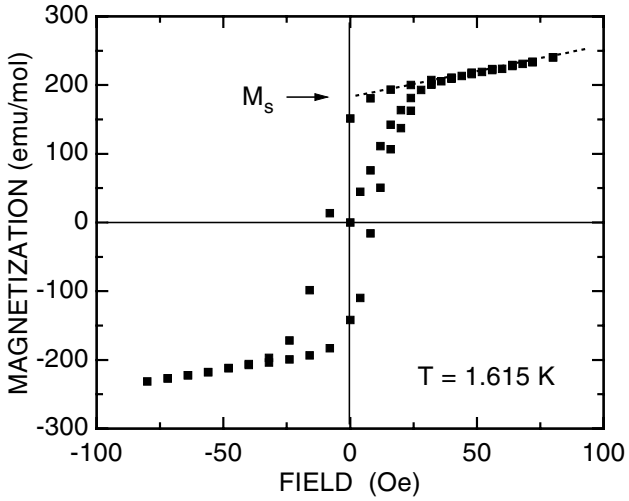

Figure 4. Hysteresis curve obtained with the magnetic field applied along the b axis. The sample was cooled down to 1.615 K in zero field and the field was then swept in the interval between + and −80 Oe. M_s is the saturated moment obtained from extrapolation of the reversible branch to zero field.

dimensional system showing canting [18], we may extrapolate the resulting $M_s(T)$ curve of figure 3 to $T = 0$. We obtain $M_s(T = 0) \approx 280$ emu mol^{-1}. The angle γ of canting can be then calculated [19, 20] giving $\gamma = \tan^{-1}[M_s(T = 0)/Ng\mu_B S] \approx 0.6^\circ$ from the c axis.

Figure 4 shows measurements of magnetization versus applied field for a sample oriented with the b axis along the applied field. The sample was cooled through T_N in zero field down to $T = 1.615$ K. The field was then cycled in the range $-80 < H < 80$ Oe. The hysteresis loop obtained is symmetric and the cycle closes for field above 30 Oe (and below −30 Oe). Above 30 Oe (below −30 Oe) the curve is completely reversible indicating that the weak component is completely saturated. The linear reversible behaviour thus observed should correspond to the susceptibility of the perpendicular antiferromagnetic underlying structure. The slope of this linear branch $M/H = 0.72$ emu mol^{-1} is in good agreement with the measured perpendicular susceptibility shown in figure 2 ($\chi_{ac} = 0.71$ emu mol^{-1}). Similar hysteresis curves were obtained at other temperatures and, as expected, this slope is temperature independent. The saturated weak net spontaneous magnetization at this temperature $M_s(T)$ can be obtained from the extrapolation of the linear reversible regions to $H = 0$ [18, 20]. We obtain $M_s(1.615\ \text{K}) \approx 180$ emu mol^{-1}. This value for M_s is plotted in figure 3. As T approaches T_N the hysteresis loop contracts and M_s tends to zero. In the interval $-30 < H < 30$ Oe of applied fields an irreversible behaviour is present. The apparent linear dependence of M as a function of H is due to progressive rotation of the weak moment along the field direction. Hysteresis curves for samples with different demagnetizing factor (N) were obtained. Samples with N differing by a factor of three gave essentially the same general behaviour apart from a change in slope of the branches of the irreversible part of the hysteresis cycle. At the temperature corresponding to the data of figure 4 the weak moment saturates above 30 Oe. The intrinsic coercive field is under 9 Oe at the temperature of the curve in figure 4. The calculated demagnetizing field for the geometry of the sample used in figure 4 is $H_d = NM(T) \approx 7$ Oe, where $M(T)$ is the magnetization per unit volume just below ±30 Oe. Similar hysteresis loops are observed with the field applied along the a^* direction. In this case a slightly larger value for M_s is obtained.

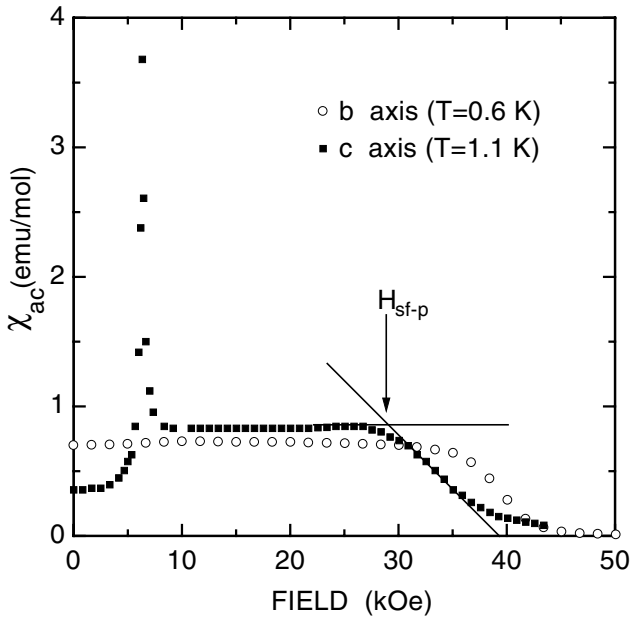

Figure 5. Typical ac susceptibility versus field curves for temperatures below T_N. In the curve with symbol (■) the field was applied along the easy axis (c axis). In the curve with symbol (○) the field was applied in the b direction. The criteria used to determine the second-order transition fields to the paramagnetic phase in both directions are schematically indicated in the figure.

4. Results in high field

To obtain the magnetic phase diagram of MnT-2 we measured χ_{ac} as function of applied field at constant T. The diagram was obtained between 0.4 and 1.83 K for field applied along the three principal magnetic axes (a^*, b and the easy c axes). Typical curves of χ_{ac} at constant temperature for H parallel to the c and b axis are shown in figure 5. The behaviour is found to be quite similar to what has been reported for other low anisotropy antiferromagnets [21]. In the curve corresponding to the field applied along the c axis the peak at $H_{sf} = 6$ kOe marks the first-order transition to the spin-flop phase. This field transition decreases with decreasing temperature. Transition from the spin-flop to the paramagnetic phase, H_{sf-p}, occurs in this curve at a field about 30 kOe. At this phase boundary the susceptibility starts to decrease due to the complete alignment of the moments in the field. The criteria to define this second-order transition field is indicated in this same figure. As the temperature approaches the bicritical point (BP), located at the confluence of the paramagnetic, antiferromagnetic and spin-flop phases, the phase boundaries to the paramagnetic phase become very steep. The transition obtained from χ_{ac} versus H traces at fixed temperature turns out to be difficult to locate because the transition region becomes very broad. The same problem is faced when we try to cross the phase boundary from the antiferromagnetic phase towards the paramagnetic phase at constant T. The phase diagram constructed from these χ_{ac} versus H traces taken at various temperatures is shown in figure 6. The solid line in this figure only suggests the boundaries close to the BP and T_N. For the phase boundaries for the two directions perpendicular to the easy axis the same problems in locating the phase boundaries were faced and the same criterion to locate the transition field was applied. Although not detailed in the region close to T_N, this phase

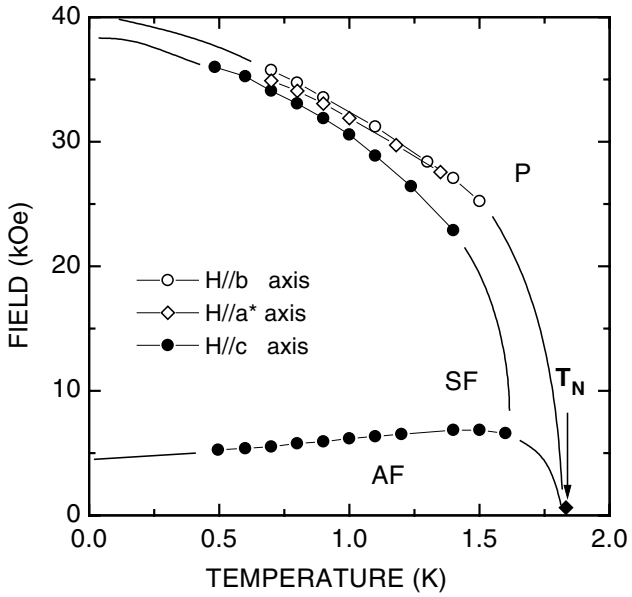

Figure 6. Magnetic phase diagram obtained for MnT-2 when the magnetic field is applied along the easy (c) axis and along the perpendicular (b and a^*) axes. The solid lines are indicative of the probable position of the phase boundaries. Due to the broadness of the transition region at temperatures above 1.5 K the position of the boundaries is difficult to establish (see text).

diagram is still useful since from it we can extract relevant parameters such as the anisotropy and exchange fields.

From the spin-flop field extrapolated to $T = 0$ K, $H_{sf}(T = 0) = 4.8$ kOe, and the value of the perpendicular susceptibility below T_N, $\chi_{ac} = 0.71$ emu mol^{-1}, the exchange (H_E) and anisotropy (H_A) parameters of the antiferromagnetic structure can be obtained. Using the mean field approximation (MFT) [22], the relations $H_{sf}^2 = 2H_E H_A - H_A^2$ and $\chi_{ac} = Ng\mu_B S/(2H_E + H_A)$ yield $H_E = 19.4$ kOe and $H_A = 0.6$ kOe. We can make an estimate of the exchange constant $Jz/k = -(H_E g\mu_B S/k) = -1.0$ K. The transition field from the spin-flop to the paramagnetic phase is given by $H_{sf-p} = 2H_E - H_A$. Using the values for anisotropy and exchange fields we obtain $H_{sf-p}(T = 0) = 38.2$ kOe. Perpendicular to the easy axis the transition field is given by $H_{perp} = 2H_E + H_A = 39.4$ kOe. The extrapolated transition fields to the paramagnetic phase at $T \to 0$ obtained from figure 6 are respectively $\approx$38 kOe and $\approx$40 kOe. These fields are in good agreement with the values obtained from H_A and H_E.

5. Conclusions

The main conclusion must be that the anomalies in the susceptibility versus temperature curves of MnT-2 characterize a transition to an antiferromagnetic state at $T_N = 1.83$ K accompanied by a canting of the spins; as a result the spins in the two sub-lattices are not exactly anti-parallel. The preferred (easy) direction for antiferromagnetic alignment is close to the c axis. The 'two' sub-lattices are slightly tilted ($\gamma \approx 0.6^\circ$ from the c axis) generating a spontaneous ferromagnetic moment in the plane perpendicular to the c axis. The weak ferromagnetism in manganese tartrate dihydrate is consistent with the DM model because the lack of inversion symmetry of the crystal field on the Mn ions.

The weak ferromagnetism and the relative value of the magnetic parameters $H_A/H_E = 0.03$ classify the manganese tartrate compound as a low anisotropy weak ferromagnet.

Acknowledgments

This research was supported by Brazilian agencies CNPq and FAPESP (grant Nos 96/12051-1 and 96/06208-5).

References

[1] Torres M E, Lopes T, Peraza J, Stockel J, Yanes A C, Gonzalez-Silgo C, Ruiz-Perez C and Lorenzo-Luis P A 1998 *J. Appl. Phys.* **84** 5729
[2] Torres M E, Yanes A C, Lopes T, Stockel J and Peraza J F 1995 *J. Cryst. Growth* **156** 421
[3] Brozek Z and Stadnicka K 1994 *Acta Crystallogr.* B **50** 59
[4] Yadava V S and Padmanabhan V M 1973 *Acta Crystallogr.* B **29** 493
[5] Valasek J 1924 *Phys. Rev.* **24** 560
[6] Yanes A C *et al* 1996 *J. Mater. Sci.* **31** 2683
[7] Lopes T *et al* 1995 *Cryst. Res. Technol.* **30** 677
[8] Dzyaloshinsky I 1958 *J. Phys. Chem. Solids* **4** 241
[9] Moriya T 1960 *Phys. Rev.* **117** 635
[10] Dekker A J 1957 *Solid State Physics* (Englewood Cliffs, NJ: Prentice-Hall)
[11] Carlin R L 1986 *Magnetochemistry* (Berlin: Springer)
[12] Bhatnagar S S, Khana M L and Nevgi M B 1938 *Phil. Mag.* **25** 234
[13] Kubecova K and Frei V 1969 *Chem. Commun.* **34** 1143
[14] Soylu H 1985 *Z. Kristallogr.* **171** 255
[15] Ramakrishnan V 1989 *Cryst. Res. Technol.* **24** 513
[16] Paduan-Filho A, Becerra C C and Palacio F 1998 *Phys. Rev.* B **58** 3197
[17] Oliveira N F Jr, Paduan-Filho A, Salinas S R and Becerra C C 1978 *Phys. Rev.* B **18** 6165
[18] Borovik-Romanov A S and Ozhogin V L 1961 *Sov. Phys.–JETP* **12** 18
[19] Palacio F, Andres M, Horne R and van Duyneveldt A J 1986 *J. Magn. Magn. Mater.* **54** 1487
[20] Petrakovskii G, Velikanov D, Vorotinov A, Balaev A, Sablina K, Amato A, Roessli B, Schefer J and Staub U 1999 *J. Magn. Magn. Mater.* **205** 105
[21] Becerra C C, Oliveira N F Jr, Paduan-Filho A, Figueiredo W and Souza M V P 1988 *Phys. Rev.* B **38** 6887
[22] de Jongh L J and Miedema A R 1974 *Adv. Phys.* **23** 1